THE JOURNAL OF PHYSICAL CHEMISTRY A

ARTICLE

pubs.acs.org/JPCA

On the Role of Nonbonded Interactions in Vibrational Energy Relaxation of Cyanide in Water

Myung Won Lee and Markus Meuwly*

Department of Chemistry, University of Basel, Klingelbergstrasse 80, 4056 Basel, Switzerland

ABSTRACT: The vibrationally excited cyanide ion (CN^-) in H_2O or D_2O relaxes back to the ground state within several tens of picoseconds. Pump−probe infrared spectroscopy has determined relaxation times of T_1 = 28 ± 7 and 71 ± 3 ps in H_2O and D_2O, respectively. Atomistic simulations of this process using nonequilibrium molecular dynamics simulations allow determination of whether it is possible at all to describe such a process, what level of accuracy in the force fields is required, and whether the information can be used to understand the molecular mechanisms underlying vibrational relaxation. It is found that, by using the best electrostatic models investigated, absolute relaxation times can be described rather more qualitatively ($T_1^{H_2O}$ = 19 ps and $T_1^{D_2O}$ = 34 ps) whereas the relative change in going from water to deuterated water is more quantitatively captured (factor of 2 vs 2.5 from experiment). However, moderate adjustment of the van der Waals ranges by less than 20% (for *NVT*) and 7.5% (for *NVE*), respectively, leads to almost quantitative agreement with experiment. Analysis of the energy redistribution establishes that the major pathway for CN^- relaxation in H_2O or D_2O proceeds through coupling to the water-bending plus libration mode.

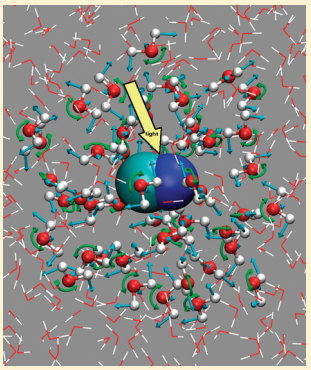

1. INTRODUCTION

The exchange of vibrational energy between molecules is important in the understanding of condensed phase chemical reactions because reaction rates and pathways are affected by the energy exchange between solvent and solute. A particularly sensitive probe of the intermolecular interactions and dynamical coupling is provided by determining rates of vibrational energy relaxation. Such studies have been carried out for a variety of systems and situations, ranging from di- and triatomic molecules in different solvents[1,2] to CO in metal carbonyl compounds[3] and heme-bound CO in proteins.[4−6] In all cases, a rich dynamical picture has emerged with vibrational relaxation times ranging from a few picoseconds to nanoseconds, depending on the solvent, ligation state (e.g., bound vs unbound diatomic), and chemical environment of the spectroscopic probe. In many cases, molecular dynamics (MD) simulations have provided considerable insight into relaxation pathways and the role of intermolecular interactions, in particular, electrostatic interactions.[4,7−9] For example, the importance of electrostatic interactions has been investigated in quite some detail for a model dipolar molecule (CH_3Cl in a united atom representation was treated as a diatomic) in polar solvent.[7,10]

A particularly well-studied system is CN^- solvated in water. Following vibrational excitation, IR-pump-IR-probe experiments have been used to determine relaxation times of the v = 1 state of CN^- in H_2O and D_2O.[1,11] In contrast to N_3^-, diatomic molecules do not display intramolecular vibrational relaxation or anharmonic coupling to intramolecular modes. Thus, relaxation is governed by intermolecular interactions and dynamical coupling between solvent and solute. It has been suggested[1] and later confirmed[11,12] that Coulomb forces are important in determining the vibrational relaxation of polar molecules in coordinating solvents, such as water. Also, CN^- has served as a model system to develop mixed quantum/classical dynamics methods to study vibrational relaxation in solvent.[13−15] Most of the simulation studies, however, were carried out with idealized interaction potentials. For example, rigid water molecules were used. On the other hand, a more elaborate four-point charge model was employed by Rey and Hynes for the CN^- molecule. The actual values of the charges were determined by trial and aimed at reproducing relaxation times and frequency shift of the CN^- vibration.[12]

Given the detailed experimental work and the previous theoretical efforts, CN^- is an ideal system to investigate the influence of intermolecular interactions on the vibrational relaxation in solvent. In the present work, the vibrational relaxation of CN^- in H_2O, D_2O, and T_2O is studied using nonequilibrium MD simulations. It has been recognized earlier that vibrational spectra and relaxation times provide a sensitive and challenging test for the intermolecular interactions used in simulations. This aspect is the focus of the present work where we ask specifically which terms in a force field are particularly sensitive to vibrational relaxation. For a more accurate description of the intermolecular interactions, distributed multipole moments (MTPs) are used to treat electrostatics.[16] Furthermore, a flexible model for the water molecules is employed.[17] To put these results into perspective, results from simulations for simpler interaction potentials are also reported.

Received: March 16, 2011
Published: May 04, 2011

There are a number of ways to obtain vibrational relaxation times from simulations. One of them uses nonequilibrium MD simulations[7] in which the bond(s) of interest are explicitly excited. By averaging over a number of nonequilibrium trajectories, a cooling time T_1 is obtained according to[18,19]

$$\frac{\overline{E_v(t)} - \overline{E_v(\infty)}}{\overline{E_v(0)} - \overline{E_v(\infty)}} = \exp(-t/T_1) \quad (1)$$

Here $E_v(t)$ is the vibrational energy at time "t", T_1 is the vibrational relaxation time, and the overbar represents an average over nonequilibrium trajectories. $\overline{E_v(\infty)}$ can be assumed to take the thermal value[20] k_BT (0.60 kcal/mol at 300 K), while $E_v(0)$ is the initial vibrational energy of the excited bond at $t = 0$.

Alternatively, T_1 can be obtained from equilibrium MD simulations through calculation of the force−force autocorrelation function $C(t) = \langle \delta F(0)\delta F(t)\rangle$ with $\delta F = F - \langle F\rangle$. For a diatomic molecule, F is the force acting on the oscillator along the bond. The correlation function $C(t)$ is related to the friction $\xi(\omega)$ through

$$\xi(\omega) = \int_{-\infty}^{\infty} dt \cos(\omega t) C(t) \quad (2)$$

and to the relaxation time $T_1^{-1} = \xi(\omega_0)/(\mu k_B T)$ where k_B is the Boltzmann constant, T is the absolute temperature, μ is the reduced mass, and ω_0 is the frequency of the oscillator.[7,20,21] If the vibrational frequency of the bond is high, the bond vibration can be treated as approximately static and constrained to its equilibrium length in simulations, only measuring fluctuation in the forces acting along the constrained bond. Results obtained using this equilibrium approach were found to be very similar to those obtained using nonequilibrium simulations with fits to eq 1.[7]

Here, nonequilibrium simulations which explicitly excite the CN^- bond and measure cooling times are used. Such an approach has previously been found to yield meaningful results for CN^- and CO relaxation in myoglobin.[9,22] In order to compare with the experimental results, the vibrational relaxation time T_1 was computed from the total vibrational energy of cyanide averaged over multiple classical MD trajectories. By comparing T_1 values obtained from simulations with and without multipole moments on the cyanide ion, it is shown that multipole moments play an important role in the simulation of vibrational energy relaxation. Furthermore, it is demonstrated that T_1 times sensitively depend on the van der Waals radii for the atoms involved and that a flexible water model is necessary for meaningful results.

As pointed out previously,[23] for a harmonic description of the system and the bath and a bilinear coupling of the two, the vibrational relaxation time T_1 computed from a classical solute−classical solvent simulation gives the same value as T_1 from a quantum solute−quantum solvent system, while quantum solute−classical solvent simulation gives slower relaxation. In very recent work,[24] it is shown that while a classical dynamics simulation can give the same relaxation time as the quantum simulation for a bilinear system−bath coupling, the relaxation times from classical and quantum simulations are different for cubic system−bath coupling. The values of the vibrational relaxation time for the amide I mode of *N*-methylacetamide (NMA) computed with classical and quantum simulations showed differences by a factor of ≈2.5 at most. For the amide I mode in NMA, vibrational relaxation can occur through the chemical bonds, similar to vibrational relaxation of CO in myoglobin (MbCO),[9] where the adjacent Fe−C_{CO} bond allows anharmonic coupling, whereas for CN^- in water no direct chemical bond is involved in the relaxation. This implies that the system−bath coupling for CN^- in water can be significantly different from that of NMA and MbCO. Thus, given these apparent differences, no straightforward scaling parameter can be inferred for the present work. We expect that the present classical dynamics simulations give relaxation times closer to those from the quantum solute−quantum solvent simulations[23] compared with the simulations where only the solute is treated quantum mechanically, while the values of the relaxation time may differ somewhat from those involving full quantum simulations, depending upon the exact nature of the system−bath coupling. The general finding that classical simulations are adequate for vibrational relaxation is also supported by recent theoretical work where quantum corrections to line shapes and echoes in vibrational and electronic spectroscopies have been investigated.[25]

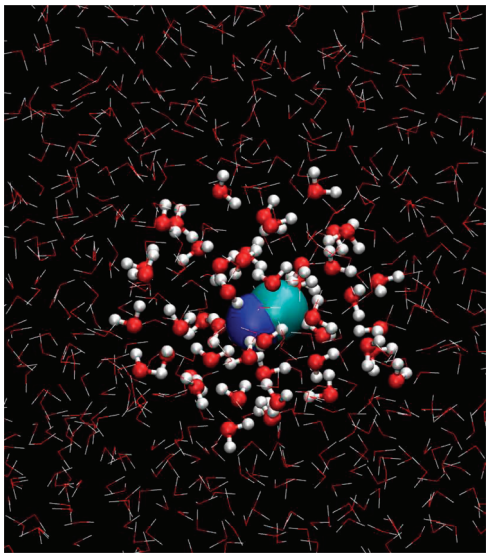

Figure 1. The simulation system used in the present work. The C and N atoms of the cyanide ion are displayed in the van der Waals spheres. The atoms of the water molecules within 7 Å from the cyanide ion are displayed as smaller spheres with the O−H bonds shown in cylinders. Other water molecules are depicted as lines.

This work is structured as follows. First the computational methods used are summarized, and the different interaction models and analysis techniques are presented. Next, results from simulations with interaction potentials of different complexity are discussed. Finally, conclusions are drawn based on comparison with experiment and previous simulations.

2. COMPUTATIONAL METHODS

All molecular dynamics (MD) simulations were carried out with the CHARMM program[26] with provisions for multipolar interactions.[16] Two preparations of the simulation system were considered:

The first consisted of one cyanide ion, CN^-, solvated in a preequilibrated cubic box of edge length 31 Å containing 997 water molecules, which amounts to 2993 atoms in total. A snapshot of this system is shown in Figure 1. These simulations were carried out with periodic boundary conditions (PBC). The nonbonded interactions (electrostatic and Lennard-Jones) were truncated at a distance of 12 Å and switched between 10 and 12 Å. Molecular

Table 1. Multipole Moments of CN^- Computed from DFT/B3LYP with aug-cc-pVQZ around the Equilibrium Bond Length[a]

	Q_{00} (e)	Q_{10} (ea_0)	Q_{20} (ea_0^2)
C	−0.447	0.973	0.318
N	−0.553	−0.698	0.963

[a] Each component is denoted by Q_u, where u represents angular momentum labels (00, 10, 11c, 11s, 20, 21c, 21s, 22c, and 22s). Only nonzero components are shown.

dynamics simulations were started in the *NPT* ensemble. An equilibration for 1.2 ns at 300 K was followed by *NVT* simulations for 200 ps using the TIP3P water model.[27] For simulations with the KKY water model (see below), an additional 200 ps of *NVT* equilibration followed for every system. Such simulations will be referred to as *NVT*(PBC,cutoff). The second preparation employed spherical boundary conditions (SBC) with a sphere of radius 19 Å, which gives a density close to 1 g/cm^3 for 997 water molecules. In these simulations no nonbonded cutoff was used, i.e., the full electrostatics was evaluated to all orders. These simulations were carried out in both, the *NVE* and *NVT* ensemble. In the following, the abbreviation *NVE*(SBC,nocutoff) or *NVT*(SBC,nocutoff) will be used. For *NVT* simulations, a Nosé-Hoover thermostat with a thermal piston mass Q = 50 kcal·mol^{-1} ps^2 was used.[28,29] Typically 20 independent simulations were carried out for every system by exciting the system (see below) at different time steps separated by up to 80 ps, and the results were averaged. In addition, simulations were carried out with a neutral system containing one K^+ ion. For comparison, previous simulations of related systems were carried out with cubic periodic boundary conditions (107 water molecules) of the charged system (no countercation), in the *NVT* ensemble and with Ewald summation and a spherical cutoff at half the box length.[12]

The stretching potential for the cyanide ion is a Morse potential

$$V(r) = D_e\{1 - \exp[-\beta(r - r_e)]\}^2 \quad (3)$$

with parameters D_e = 237.5 kcal/mol, β = 2.283 Å^{-1}, and r_e = 1.172 Å.[30] The Lennard-Jones (LJ) parameters used for the cyanide ion were ε = 0.105 kcal/mol and $r_{min}/2 = \rho$ = 1.926 Å for the C atom and ε = 0.069 kcal/mol and ρ = 1.830 Å for the N atom, which were taken from the universal force field (UFF).[31] For the electrostatic interactions a distributed multipole analysis (DMA) is employed.[32] The multipole moments for CN^- are calculated from density functional theory (DFT) calculations at the B3LYP/aug-cc-pVQZ level. The Gaussian03 suite of programs[33] was used to obtain the SCF wave functions, from which the charges (q), dipole ($\vec{\mu}$), and quadrupole (Θ) moments on the C and N atoms were calculated through the GDMA program.[32] Each multipole moment Q was calculated on a grid ranging from 0.9 to 1.1r_e with a step size of 0.1r_e, where r_e = 1.177 Å is the experimentally determined equilibrium bond length.[34] To include variation of the multipole moments during vibration, all moments were fit to a linear function $Q(r) = a + br$, which proved sufficiently accurate. The values of all nonzero components up to quadrupole are summarized in Table 1. To describe the orientations of the atomic multipole moments with respect to the global Cartesian coordinate system, reference axis systems are assigned to each molecule and the interactions are transformed in each step to the global axis system. For the cyanide anion, which is isoelectronic with carbon monoxide, the charge distribution is axially symmetric and only one axis is required. Here, the z-axis is chosen, which is parallel to the molecular axis.

For water, two different models were used. One was a standard TIP3P potential,[27] for which the bond lengths were constrained by applying SHAKE[35,36] and a 1 fs time step was used in the simulations. Furthermore, a flexible water model based on the parametrization by Kumagai, Kawamura, and Yokokawa (KKY)[17] was used with different charge models and a smaller time step of 0.4 fs to account for the flexible O−H bonds and H−O−H angle. The functional form of the KKY potential for the stretching and bending energies is

$$\begin{aligned} E_{str} &= D\{\exp[-2\beta(r - r_0)] - 2\exp[-\beta(r - r_0)]\} \\ &= D\{1 - \exp[-\beta(r - r_0)]\}^2 - D \end{aligned} \quad (4)$$

and

$$\begin{aligned} E_{bend} &= -f_k\sqrt{k_1k_2}\{\cos[2(\theta - \theta_0)] - 1\} \\ &= 2f_k\sqrt{k_1k_2}\sin^2(\theta - \theta_0) \end{aligned} \quad (5)$$

where $k_i = 1/\{\exp[g_r(r_i - r_m)] + 1\}$, in which r_i is the distance of one O−H bond of the water molecule and g_r and r_m are parameters given in Table 2. With the KKY, electrostatic interactions were either TIP3P charges or multipole moments previously determined,[37] which were independent of the geometry of the water molecule. For the Lennard-Jones parameters ρ and ε, those of the TIP3P model were used in all simulations.

Infrared Spectra. The infrared (IR) spectrum from MD simulations is calculated from the Fourier transform of the dipole moment autocorrelation function $C(t)$ which is accumulated over 2^n time origins, where n is an integer such that 2^n corresponds to between 1/3 and 1/2 of the trajectory, with the time origins separated by 0.8 fs. $\hat{C}(\omega)$, which is the Fourier transform of $C(t)$, is computed using a fast Fourier transform (FFT) with a Blackman filter for the reduction of noise.[38] The final infrared absorption spectrum $A(\omega)$ is then calculated from

$$A(\omega) = \omega\{1 - \exp[-\hbar\omega/(k_BT)]\}\hat{C}(\omega) \quad (6)$$

where k_B is the Boltzmann constant and T is the absolute temperature in kelvin.

Vibrational Excitation. For the vibrational excitation of CN^- from E_0 to E_1 with $E_1 - E_0$ = 5.94 kcal/mol,[11] the velocities of the C and N atoms were changed without affecting the bond distance at the moment of excitation. This results in adding a fixed amount of energy corresponding to the experimental vibrational excitation ($E_1 - E_0$). In order to add energy by changing the velocities, the velocities of the C and N atoms were decomposed into the components corresponding to the translational motion of the center of mass and those of the internal motion. The velocity components corresponding to the internal motion were further decomposed into a term corresponding to the vibration and two other terms corresponding to the rotation. Only the velocity component corresponding to the vibration was increased to add the desired vibrational kinetic energy. The changes in the velocities of the C and N atoms can be computed by

$$m_C\Delta v_C = -\mu(v_C - v_N) \pm \sqrt{\mu^2(v_C - v_N)^2 + 2\mu\Delta E} \quad (7)$$

dx.doi.org/10.1021/jp202503m |J. Phys. Chem. A 2011, 115, 5053–5061

Table 2. Parameters for Water Potential Reported in the Work of Kumagai et al.[17] and Used in This Work, Together with the Harmonic Frequencies Computed from Them[a]

	D (E_h)	β (a_0^{-1})	r_0 (a_0)	f_k (E_h)	θ_0 (deg)	r_m (a_0)	g_r (a_0^{-1})	ν_1	ν_2	ν_3
KKY[b]	0.120	1.45	1.55	2.5×10^6	99.5	2.65	3.7	3720	1525×10^4	3763
this work	0.120	1.44	1.81	0.0388	99.5	2.65	3.7	3689	1595	3724

[a] Atomic units are used for D, β, r_0, f_k, r_m, and g_r. θ_0 is given in degrees and frequencies (ν_1, ν_2, and ν_3) in cm^{-1}. [b] The literature data were converted to atomic units from the following parameters: D = 75.0 kcal/mol, β = 2.74 $Å^{-1}$, r_0 = 0.82 Å, $f_k = 1.1 \times 10^{-11}$ J, r_m = 1.40 Å, and g_r = 7.0 $Å^{-1}$.

and

$$m_N \Delta v_N = \mu(v_C - v_N) \mp \sqrt{\mu^2(v_C - v_N)^2 + 2\mu\Delta E} \quad (8)$$

where m_α is the mass of atom type α, Δv the change in velocity due to vibrational excitation, v the velocity before excitation, μ the reduced mass, and ΔE the energy corresponding to the vibrational excitation, $E_1 - E_0$.

The vibrational relaxation time T_1 is obtained from eq 1[18] by fitting the vibrational energy of CN^- after excitation. The thermal value of 0.60 kcal/mol at 300 K was used for $\overline{E_v(\infty)}$, and 5.94 kcal/mol was used for $E_v(0) - \overline{E_v(\infty)}$ from the experimental vibrational frequency of 2079 cm^{-1} for $^{12}C^{14}N^-$ in water.[11]

Analysis. The energy release from vibrational deexcitation of CN^- was analyzed by decomposing the total energy into different components, i.e., the energy of the cyanide ion was decomposed into potential and kinetic energy, and the latter was further decomposed into the translational, rotational, and vibrational components. The sum of potential and vibrational kinetic energy of CN^- was monitored at each step. For the water molecules, the kinetic energy was decomposed into energies describing the translational (E_T), rotational (E_R), and vibrational (E_V) degrees of freedom. This was done by transforming a space-fixed Cartesian coordinate system into a molecule-fixed normal coordinate system.[39] For E_T

$$Q_k = N_k \sum_{\alpha=1}^{3} m_\alpha^{1/2} q_{3\alpha - 3 + k} \quad (9)$$

where Q_k with k = 1, 2, or 3 corresponds to translational motion in the x, y, or z-directions, N_k values are the normalization constants, m_α the mass of atom α, and q_i the mass-weighted Cartesian displacement coordinates, i.e., $q_1 = m_1^{1/2}\Delta x_1$, $q_2 = m_1^{1/2}\Delta y_1$, ⋯, $q_9 = m_3^{1/2}\Delta z_3$.

For E_R

$$Q_k = N_k \sum_{\alpha=1}^{3} m_\alpha^{1/2} \sum_{i=1}^{3}\sum_{j=1}^{3} \varepsilon_{ijk'} r_{3\alpha-3+i}\ q_{3\alpha-3+j} \quad (10)$$

where Q_k with k = 4, 5, or 6 corresponds to rotational motion around the x, y, or z-directions, $\varepsilon_{ijk'}$ is the Levi−Civita symbol with $k' = k - 3$, and r_i the coordinates of the equilibrium positions, i.e., $r_1 = x_1^{(0)}$, $r_2 = y_1^{(0)}$, ⋯, $r_9 = z_3^{(0)}$.

The three vibrational modes are described by

$$Q_k = \sum_{i=1}^{9} l_{ik} q_i \quad (11)$$

where Q_k values are normal coordinates of vibrations (k = 7, 8, or 9) and l_{ik} are the eigenvectors of the Hessian matrix with respect to the mass-weighted Cartesian coordinates and satisfy $\Sigma_i l_{ik}^2 = 1$. Then, each component of the kinetic energy can be obtained from

$$T_k = \frac{1}{2}\dot{Q}_k^2 \quad (12)$$

3. RESULTS AND DISCUSSION

The parameters reported in the work of Kumagai et al.[17] and those used in the present work are summarized in Table 2. D and θ_0 used here are identical to the original KKY parameters. The bending parameter (f_k) has been changed by several orders of magnitude to match the experimental frequency (see below), whereas the value of β (stretching) has been changed only slightly (≈1%). For r_0, the TIP3P value of 0.9572 Å was used to allow direct comparison with the simulations using the TIP3P water model. With these parameters, the average of the symmetric and asymmetric stretching frequencies, $(\nu_1 + \nu_3)/2$, matches the experimental value in the gas phase (ν_1 = 3657 cm^{-1} and ν_3 = 3756 cm^{-1}).[40] Fitting to the average frequency was done because it turned out to be difficult to match individual frequencies. The value for f_k was also adjusted to match the experimental bending frequency, ν_2 = 1595 cm^{-1}. To calculate gas-phase frequencies from the KKY potential, the numerical Hessian was constructed from the gradients computed analytically at the optimized geometry, which yields 3689, 1595, and 3724 cm^{-1} (ν_1, ν_2, and ν_3). These values are close to the experimental values of 3657, 1595, and 3756 cm^{-1}.[40] The vibrational frequencies of gas-phase H_2O calculated from the original KKY parameters (see Table 2) are 3720, 1525×10^4, and 3763 cm^{-1}. As pointed out previously,[41] the value of f_k from the original KKY parametrization seems to be several orders of magnitude too large and overestimates the bending frequency. This is probably related to the fact that the parameters were fitted to thermodynamic rather than spectroscopic data.[17,42] As KKY is an anharmonic potential, it is also of interest to calculate the fundamentals directly from the dipole moment correlation function from an explicit MD simulation of one water molecule. This leads to 3676, 1586, and 3714 cm^{-1} for the three fundamentals.

The computed frequency for CN^- from the dipole moment autocorrelation function with the Morse parameters (see Methods) of the cyanide ion in H_2O was 2163 cm^{-1}. By changing the value from β = 2.283 (see Methods) to β = 2.101 $Å^{-1}$ for the CN^- Morse potential, the calculated frequency of CN^- changed accordingly to 1997 cm^{-1}, which is close to the experimentally determined value of 2079 cm^{-1} measured in H_2O.[11] Experimental data on the gas phase frequency of CN^- is rare. The value from the work of Bradforth et al.[34] is 2035 ± 40 cm^{-1}.

In the following, CN^- vibrational relaxation is studied by using increasingly accurate interaction models. This is particularly relevant to more fundamentally understand which types of interactions primarily affect the relaxation process and its efficiency. This is one of the particular advantages of atomistic simulations. Thus, different levels of complexity for describing the CN^- anion and the surrounding water molecules are combined, scrutinized, and analyzed in the following. To characterize the relative changes in T_1 on the charge model and water-parametrization, NVT(PBC,cutoff) simulations were carried out. In the section that discusses the sensitivity to Lennard-Jones parameters, both NVT(PBC,cutoff)

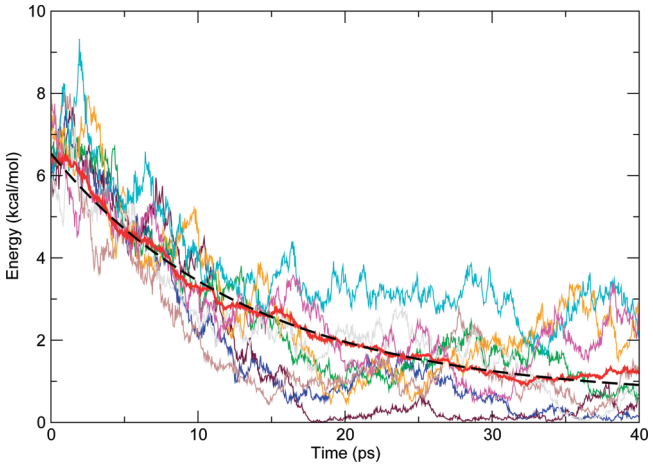

Figure 2. The vibrational energy of the cyanide ion in H_2O after vibrational excitation. Red solid curve is the averaged energy over 20 trajectories and black dotted line is obtained from the fitting of the red curve to an exponential function. Raw vibrational energies of CN^- for 8 independent trajectories are shown as well.

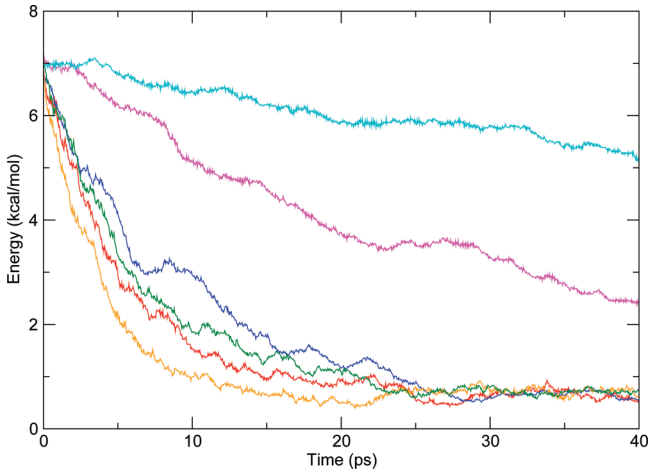

Figure 3. The averaged vibrational energy of the cyanide ion in H_2O and D_2O with $\beta = 2.101$ Å^{-1} and $f_k = f_{k,0}$, calculated with (1) charges plus dipole and quadrupole moments (CDQ), (2) charges and dipole moments (CD), and (3) charges only (C), on the C and N atoms of the cyanide ion. Vibrational relaxation accelerates with inclusion of higher multipole moments. Red curve is for (CDQ, H_2O), blue for (CDQ, D_2O), orange for (CD, H_2O), green for (CD, D_2O), magenta for (C, H_2O), and cyan for (C, D_2O).

and *NVE*(SBC, nocutoff) are used and compared. It is found that the changes in T_1 between these two treatments are typically small (around 20%) and relative changes $T_1^{H_2O}/T_1^{D_2O}$ in going from H_2O to D_2O as a solvent are largely unaffected.

Quadrupolar CN^- with KKY Water and Point Charges. The total vibrational energy of CN^- as a function of time for CN^- in H_2O is shown in Figure 2 when the cyanide ion is excited at $t = 0$. The average vibrational energy of the cyanide ion was obtained by averaging over 20 independent trajectories. For clarity, only 8 separate trajectories are shown in the figure, together with the ensemble average over 20 trajectories and the exponentially decaying fit to the simulation data, which yields T_1 = 13.6 ps. For all other simulations, similar relaxation curves were found.

Point-Charge, Dipolar, and Quadrupolar CN^- with KKY Water and Point Charges. MD simulations were carried out with different electrostatic interactions of CN^- to further investigate the effect of multipole moments. Three cases for CN^- in H_2O and D_2O are compared in Figure 3: (1) the cyanide ion described with charge, dipole, and quadrupole moments (CDQ), (2) with charge and dipole moments (CD), and (3) with charges (C) only on the C and N atoms. As shown in Figure 3, vibrational relaxation of CN^- with the charge only is much slower (T_1 = 36 ps for H_2O and 205 ps for D_2O) compared to simulations including dipole moments on the C and N atoms (T_1 = 3.9 ps for H_2O and 7.1 ps for D_2O), which accelerate vibrational relaxation significantly. Quadrupole moments have a smaller effect on (5.8 ps for H_2O and 9.1 ps for D_2O), compared to adding dipole moments.

Quadrupolar CN^- with Quadrupolar KKY Water. We also investigated the effect of multipole moments on the water molecules in view of the vibrational relaxation of CN^- by performing MD simulation with charges, dipole, and quadrupole moments on the oxygen atoms of the water molecules together with charges on the hydrogen atoms. This leads to relaxation times of 9.7, 19.0, and 6.0 ps for CN^- in H_2O, D_2O, and T_2O, respectively, which are longer than those obtained with MTP only on the cyanide ion (5.8, 9.1, and 1.2 ps), see Table 3.

Bonded Terms. Because CN^- was parametrized with respect to gas phase data, simulations with varying Morse parameters were also carried out. It is expected that the CN^- equilibrium bond length does not change appreciably in going from the gas phase to solution. Furthermore, the dissociation energy does not strongly influence low-energy processes such as the vibrational relaxation (v = 1) → (v = 0) studied here. Therefore, further attention was focused on the steepness parameter β. For β = 1.918, 2.101, 2.283, and 2.398 Å^{-1}, the CN^- fundamental from MD simulation is at 1830, 1997, 2163, and 2269 cm^{-1}, compared to 2035 ± 40 cm^{-1} from experiment.[34] Again, relaxation times were calculated from ensemble averages over 20 independent simulations for all different values for β for CN^- in H_2O, D_2O, and T_2O and the result is shown in Figure 4. It is found that the rate of vibrational relaxation sensitively depends on β used in the Morse potential. As $\beta = 2.283$ Å^{-1}, which was obtained from the quantum chemical calculations, gives a slightly higher vibrational frequency (ν_{CO} = 2163 cm^{-1}) in the MD simulations than the experimental value, $\beta = 2.101$ Å^{-1} is used in the following which gives ν_{CO} = 1997 cm^{-1}. Since the vibrational frequencies for values too different from β = 2.283 Å^{-1} do not reproduce the experimentally determined CN^- stretching frequency, this sensitivity should probably only be used to fine-tune force field parameters (see Discussion).

Similar considerations apply to the parametrization of the flexible water model. As the vibrational energy of CN^- is dissipated into solvent modes and the rate for vibrational energy transfer from CN^- to the solvent depends on the frequencies of CN^- and of the solvent molecules, details of the water parametrization possibly affect the vibrational relaxation time of CN^-. Given that the water bending mode frequency is closest to the CN^- stretch, the sensitivity of vibrational relaxation with respect to the bending force constants f_k of water was considered in more detail. Therefore, simulations were also carried out with three different values for f_k including $f_{k,0}$ (which reproduces the gas phase bending frequency), $0.95f_{k,0}$ and $1.05f_{k,0}$. The dependence of T_1 on f_k is considerably weaker than on β of the CN^- Morse potential, with typical changes of T_1 by less than 5%.

dx.doi.org/10.1021/jp202503m |*J. Phys. Chem. A* 2011, 115, 5053–5061

Table 3. Vibrational Relaxation Time (T_1) in Picoseconds for the Cyanide Ion Obtained from Various Simulations[a]

MTP	CN^-	CN^-	CN^-	CN^-/water	CN^-/water	CN^-/water	CN^-/water	CN^-/water	CN^-/water	exp[11]
ρ^C	1.926	1.926	2.118	1.926	1.926	2.118	2.311	2.070	2.214	
ρ^N	1.830	1.830	2.013	1.830	1.830	2.013	2.196	1.967	2.105	
ensemble	*NVT*	*NVE*	*NVT*	*NVT*	*NVE*	*NVT*	*NVT*	*NVE*	*NVE*	
boundary	PBC	SBC	PBC	PBC	SBC	PBC	PBC	SBC	SBC	
H_2O	5.8 ± 0.7	5.3 ± 0.8	14.1 ± 1.6	9.7 ± 1.2	11.9 ± 1.3	18.8 ± 1.9	26.8 ± 3.0	22.1 ± 2.2	36.2 ± 6	28 ± 7 ps
D_2O	9.1 ± 1.1		26.4 ± 5.7	19.0 ± 2.6	22.4 ± 2.9	33.8 ± 3.2	81.6 ± 11	67.5 ± 11	126 ± 16	71 ± 3 ps
T_2O	1.2 ± 0.1			6.0 ± 0.6		9.7 ± 1.0				

[a] Comparison of T_1 times from *NVT* or *NVE* simulations with and without MTP on water and different values for $\rho = r_{min}/2$ for the LJ potential. In all cases, $\beta = 2.101$ Å^{-1} was used. Each T_1 value was computed by fitting the average energy of CN^- over 20 trajectories to eq 1. Experimental data are those from the work of Hamm et al.[11] and given in the last column. The errors of the computed T_1 times were estimated by calculating the standard deviation of T_1 computed from bootstrapping by averaging over all selections of 10 out of the 20 trajectories.

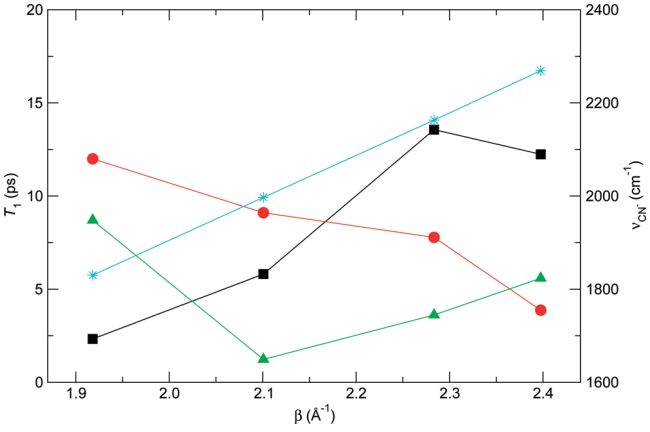

Figure 4. The vibrational relaxation time, T_1, of CN^- with different β values in the Morse potential (see eq 3) for simulations in H_2O (black), D_2O (red), and T_2O (green). MTPs only on CN^-, KKY water model, and ρ values of C and N from UFF[31] were used. The rate of vibrational relaxation depends sensitively on the potential parameters used in the simulation. The vibrational frequencies of CN^- computed from the MD simulations with various β values are shown in cyan.

Lennard-Jones Parameters. Lennard-Jones parameters were found to sensitively affect vibrational relaxation. To better understand their influence, both *NVE*(SBC) and *NVT*(PBC) simulations for varying well depth (ε) and range (ρ) parameters for the C and N atoms were carried out. The dependence of T_1 on ε was small: with increases of ε by a factor of 2−4, T_1 changed by less than 2-fold. Contrary to that, the van der Waals range ρ greatly affects T_1.

First, *NVT* and *NVE* were compared. For this, SBC simulations with $\beta = 2.101$ Å^{-1} and DMA up to quadrupoles on CN^-, and KKY and point charges on water for the neutral system (see Methods) were carried out which yield $T_1 = 5.3$ ps for *NVE* vs $T_1 = 5.1$ ps for *NVT*. This compares with $T_1 = 5.8$ ps from *NVT* with PBC without K^+. Next, to quantify the effect of the countercation, simulations of CN^- in water with and without the K^+ ion using *NVE*(SBC,nocutoff) were carried out. The vibrational relaxation time of CN^- without the K^+ ion was $T_1 = 5.8$ ps while with the K^+ ion present it was $T_1 = 5.3$ ps. This suggests that the effect of the countercation on the relaxation times is small. Finally, the sensitivity on the cutoff radius was assessed by comparing *NVE*(SBC) simulations without K^+. The relaxation time of CN^- was $T_1 = 5.8$ ps for *NVE*(SBC,nocutoff) and $T_1 = 4.6$ ps for *NVE*(SBC,cutoff). In conclusion, the electrostatic cutoff is found to affect the results by up to 20% whereas differences between *NVE* and *NVT* on one hand and the neutral and charged system on the other hand are smaller.

After these considerations, the dependence of T_1 on the van der Waals ranges of C and N was studied more systematically. The results are summarized in Table 3. Both, simulations in *NVT*(PBC,cutoff) with electrostatic cutoff and *NVE*(SBC, nocutoff) with infinite electrostatic cutoff were carried out for ρ values for the C and N atoms of 1.926 and 1.830 Å, respectively,[31] and values modified by up to 20%. Increasing ρ by 10% changes T_1 from 5.8 to 14.1 ps for H_2O and from 9.1 to 26.4 ps for D_2O (see Table 3) in *NVT*(PBC) and MTP only on CN^- and not on water. Thus, a 10% change in ρ affects T_1 by a factor of almost 3. Including MTP on the water molecules as well, the relaxation times in *NVT*(PBC) and *NVE*(SBC) are $T_1 = 9.7$ and 11.9 ps for H_2O and 19.0 and 22.4 for D_2O, respectively. Increasing ρ again by 10% leads to $T_1 = 18.8$ ps and 33.8 in *NVT*(PBC) for H_2O and D_2O, respectively. One thus finds that in all cases CN^- relaxation in H_2O is shorter by a factor of 2 or more than in D_2O, which is in qualitative agreement with experimental values of $T_1 = 28 \pm 8$ ps and $T_1 = 71 \pm 3$ ps.[11] However, the absolute T_1 is too short in both solvents.

Therefore, ρ was considered an adjustable parameter, and for *NVT*(PBC,cutoff) and *NVE*(SBC,nocutoff) the changes required in ρ to match experimental relaxation times were determined separately. Increasing (ρ^C, ρ^N) by 20% to (2.311, 2.196) Å, relaxation times in *NVT*(PBC,cutoff) are $T_1^{H_2O} = 26.8$ ps and $T_1^{D_2O} = 81.6$ ps. For *NVE*(SBC,nocutoff) the required change is smaller, namely, 7.5% or (ρ^C, ρ^N) = (2.070, 1.967) Å and yields $T_1^{H_2O} = 22.1$ ps and $T_1^{D_2O} = 67.5$ ps. Thus in the two ensembles changes between 7.5% and 20% reproduce the experimental data. This can be compared to van der Waals ranges used in different force fields. For the C and N atoms they are $\rho = 1.70$ and 1.55 Å according to the compilation of Bondi.[43] Other values in the literature are $\rho = 1.90$ Å for C from simulations of a polyethylene crystal,[44] whereas ρ for different carbon atom types in the CHARMM22 force field ranges from 1.80 to 2.275 Å and $\rho = 1.85$ Å for nitrogen. Finally, the AMBER parametrization uses $\rho = 1.91$ Å for C and $\rho = 1.82$ Å for N. Thus, for carbon atoms ρ can range from 1.70 to 2.28 Å (relative change of 25%) and for nitrogen atoms values between 1.55 and 1.85 (relative change of 16%) can be found depending on the source. Here, a moderate

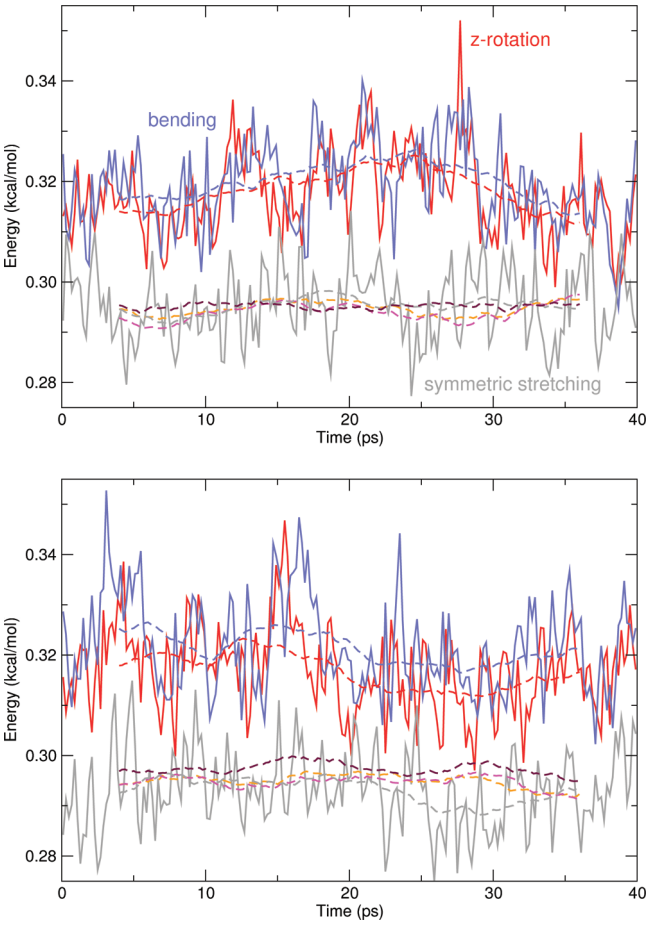

Figure 5. The rotational and vibrational energy components of H_2O (upper panel) and D_2O (lower panel) as a function of time just after the vibrational excitation of CN^-, averaged over the water molecules within 7.0 Å from the cyanide ion. MTPs only on CN^-, $\beta = 2.101$ Å^{-1} for CN^-, and KKY water model. Orange, magenta, and red curves are for rotations around the *x*, *y*, and *z*-directions, and blue, gray, and maroon curves are for bending, symmetric stretching, and asymmetric stretching vibrations. Running averages are shown in dotted lines, and the data for some components before the running average are shown in solid lines.

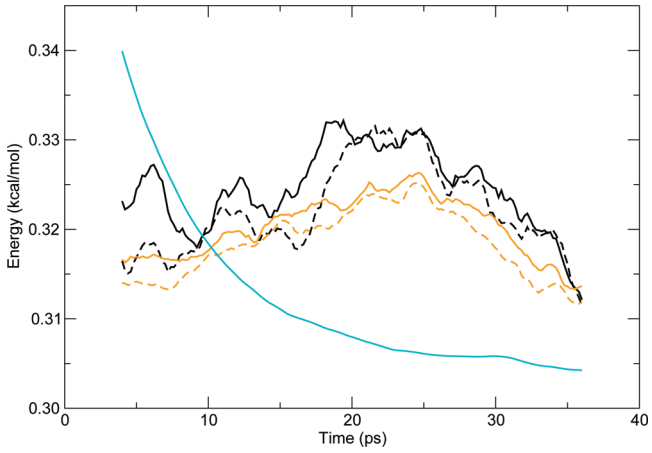

Figure 6. Averaged energy components per H_2O molecule for the rotation in the *z*-direction (dotted lines) and the bending mode (solid lines) of H_2O, within 4.0 Å (black) and 7.0 Å (orange) from the cyanide ion, respectively, just after vibrational excitation of CN^-. For comparison, the total vibrational energy of the cyanide ion is also displayed in cyan after rescaling ($0.01E_{vib} + 0.3$).

increase in ρ for C and N atoms compared to the initial values from the universal force field (UFF)[31] is found to reproduce experimental T_1 times. The actual ρ values are well within the variations found in different force fields. This applies to simulations with *NVE*(SBC,nocutoff) which is probably the technically more appropriate ensemble for investigating vibrational relaxation. However, it should be noted that previous simulations also employed *NVT*(PBC) for the same purpose[12] and that the changes predicted from *NVT*(PBC,cutoff) are still within variations found in different force fields.

Energy Flow. To analyze energy flow, the average potential and kinetic energies were computed from simulations with *NVT*(PBC,cutoff,no K^+) and with *NVE*(SBC,nocutoff,K^+). For the latter, see below. Potential energy components for the water stretching and bending parts were computed separately, and the kinetic energy was decomposed into translation (T), rotation (R), and vibration (V). As required by the equipartition theorem, each component of (E_T,E_R,E_V) has an average value of ≈0.30 kcal/mol at T = 300 K. Each energy component was averaged over 20 trajectories and over water molecules within a sphere of given radius around the center of mass of the cyanide ion. The sphere included approximately 50 water molecules when the radius was 7.0 Å and 10 molecules with a radius of 4.0 Å. Energies $E_R(t)$ and $E_V(t)$ for the water molecules around the cyanide ion are shown in Figures 5 and 6. The three E_R components correspond to rotations around the molecule-fixed *x*, *y*, and *z* axes for a water molecule in the *xy* plane with its C_{2v} axis parallel to the *y* axis. The three components of E_V correspond to the bending, symmetric stretching, and asymmetric stretching modes.

To better understand the relaxation *mechanism*, the internal energies of the surrounding water molecules are analyzed in more detail. For vibrational relaxation of the cyanide ion to be effective, the water molecules closest to the ion should readily absorb the liberated energy. This is best achieved if the CN^- vibrational frequency (2079 cm^{-1})[11] matches fundamentals or combination bands of the surrounding water. For liquid H_2O, the combination mode (bending + libration) is observed experimentally at 2127.5 cm^{-1},[45] which is close to the fundamental of cyanide. Figures 5 and 6 report the average energies in different degrees of freedom of the water molecules from the MD simulations after vibrational excitation of CN^- with MTPs only on CN^-, β = 2.101 Å^{-1} for CN^-, and the KKY water potential. Most of the curves oscillate around the thermal value of ≈0.30 kcal/mol as expected from the equipartition theorem. However, the rotational energy around the *z*-direction (red) and the bending mode (blue) differ from the equilibrium value. Initially, they increase due to coupling to the excited CN^- vibration. They reach a maximum 20 ps after excitation, after which the energy components sharply start to approach the thermal value. This indicates that the excess vibrational energy of CN^- is preferentially absorbed by these modes, which is what is expected based on the frequency matching between the CN^- vibration and the combination mode of bending and libration for liquid H_2O. When the energies of these two modes were monitored for water molecules within spheres of different radii around the ion, it was found that for smaller radii (4 Å) the energy increases earlier after vibrational excitation than for larger radii (7 Å). In the latter case,

dx.doi.org/10.1021/jp202503m |*J. Phys. Chem. A* 2011, 115, 5053–5061

averaging is carried out over more water molecules, which dilutes the effect and leads to less pronounced and retarded effects.

The same analysis was carried out for *NVE*(SBC,nocutoff,K^+) simulations. The energy components of H_2O molecules within 7 Å were considered and it is found that the rotation around the *z*-direction and the bending mode of H_2O are mainly involved in the energy transfer from the vibrationally excited CN^- ion. This is in agreement with the above *NVT*(PBC,cutoff,no K^+) simulations.

A similar analysis was performed for D_2O within 7 Å from the CN^- ion. The rotational and vibrational energy components of D_2O are shown in the lower panel of Figure 5. As for H_2O, the rotational mode in the *z*-direction and the bending mode of D_2O are preferred in the vibrational relaxation of CN^-. When considering the data in more detail, it is found that the *mechanism* for vibrational energy relaxation of CN^- in D_2O is probably different from that in H_2O. The kinetic energy component of rotation in the *z*-direction (red curves in Figure 5) and that of the bending mode (blue curves in Figure 5) of water change in parallel to each other for H_2O, while the correlation is weaker in the case of D_2O. For D_2O, the frequency of the bending mode is 1178 cm^{-1}, so the first overtone is close to the fundamental of the cyanide, which would facilitate the bending mode of D_2O to absorb the vibrational energy of the cyanide. The combination mode of D_2O at 1555 cm^{-1} would also be involved in energy transfer. As recently shown,[46] the symmetric stretching mode of D_2O (gas phase frequency 2669 cm^{-1}) has a wide low frequency wing in the liquid phase, which can absorb the vibrational energy of the cyanide. Considering the gray curve in the lower panel of Figure 5 corresponding to the vibrational kinetic energy of D_2O symmetric stretching mode, a small increase can be discerned between 3 and 5 ps, which indicates that this mode absorbs some energy from the vibration of the cyanide.

4. CONCLUSION

In the present work, relaxation of a vibrationally excited CN^- ion in water and some of its isotopic variants has been investigated by atomistic simulations with force fields of different quality. It was found that with fully flexible force fields and accurate representations of the nonbonded interactions between the molecules, quantitative agreement with experimentally determined relaxation times can be obtained.

To establish that a flexible water model is required, simulations with a rigid TIP3P model were also carried out (20 trajectories, 1 ns in length). They found only very slow (several hundred picoseconds) vibrational relaxation of CN^- in H_2O with T_1 = 574 ps. This contrasts with facile and realistic relaxation times from simulations with a flexible water model based on the KKY potential. Thus, allowing for flexible internal degrees of freedom in the solvent is essential for realistic vibrational relaxation times of the solute.

A remarkable finding of the present work is that the calculated T_1 times sensitively depend on the force field parametrization, in particular the Lennard-Jones ranges. Increasing ρ by up to 7.5% in *NVE*(SBC,nocutoff) simulations leads to longer relaxation times by a factor of 4−5. This can be qualitatively understood by noting that for larger ρ the distance between the solvent water molecules and CN^- will be larger on average which, in turn, leads to reduced electrostatic interactions and hence less efficient vibrational energy transfer. The current work suggests that ρ values for the C and N atoms of 2.070 and 1.967 Å are suitable for simulations in full solvation.

The possibility to refine particular force field parameters (here van der Waals ranges) from ensemble-averaged atomistic simulations is an attractive extension over more conventional parametrization strategies. Similar efforts have been undertaken for NMR scalar coupling constants, for which partial charges of atoms involved in hydrogen bonds were refined.[47−49]

In conclusion, the present work establishes that for meaningful atomistic simulations of vibrational relaxation of simple ions in solution, fully flexible force fields should be employed. Electrostatics beyond simple point charges is mandatory (for CN^- the effect of the atomic dipole is most pronounced), and the actual relaxation times depend sensitively on the van der Waals ranges. Combining all these insights allows us to capture the rapid relaxation of CN^- in H_2O and D_2O, to almost quantitatively describe the relative change of a factor of 2.5 for $T_1^{D_2O}/T_1^{H_2O}$ observed experimentally, and to understand the mechanism for vibrational relaxation whereby CN^- vibrational energy is primarily transferred to the water-bending and librational modes.

AUTHOR INFORMATION

Corresponding Author

*E-mail: m.meuwly@unibas.ch.

ACKNOWLEDGMENT

The authors gratefully acknowledge financial support from the Swiss National Science Foundation through Grants 200021-117810 (to M.M.) and 200021-124936 (to the NCCR Molecular Ultrafast Science and Technology (MUST)). We thank Professor P. Hamm for stimulating discussions.

REFERENCES

(1) Heilweil, E. J.; Doany, F. E.; Moore, R.; Hochstrasser, R. M. *J. Chem. Phys.* **1982**, *76*, 5632–5634.
(2) Li, M.; Owrutsky, J.; Sarisky, M.; Culver, J. P.; Yodh, A.; Hochstrasser, R. M. *J. Chem. Phys.* **1993**, *98*, 5499–5507.
(3) Heilweil, E. J.; Cavanagh, R. R.; Stephenson, J. C. *Chem. Phys. Lett.* **1987**, *134*, 181–188.
(4) Sagnella, D. E.; Straub, J. E.; Jackson, T. A.; Lim, M.; Anfinrud, P. A. *Proc. Natl. Acad. Sci. U.S.A.* **1999**, *96*, 14324–14329.
(5) Owrutsky, J. C.; Li, M.; Locke, B.; Hochstrasser, R. M. *J. Phys. Chem.* **1995**, *99*, 4842–4846.
(6) Mizutani, Y.; Kitagawa, T. *Chem. Rec.* **2001**, *1*, 258–275.
(7) Whitnell, R. M.; Wilson, K. R.; Hynes, J. T. *J. Phys. Chem.* **1990**, *94*, 8625–8628.
(8) Egorov, S. A.; Skinner, J. L. *J. Chem. Phys.* **1996**, *105*, 7047–7058.
(9) Devereux, M.; Meuwly, M. *J. Phys. Chem. B* **2009**, *113*, 13061–13070.
(10) Whitnell, R. M.; Wilson, K. R.; Hynes, J. T. *J. Chem. Phys.* **1992**, *96*, 5354–5369.
(11) Hamm, P.; Lim, M.; Hochstrasser, R. M. *J. Chem. Phys.* **1997**, *107*, 10523–10531.
(12) Rey, R.; Hynes, J. T. *J. Chem. Phys.* **1998**, *108*, 142–153.
(13) Bastida, A.; Zuniga, J.; Requena, A.; Miguel, B. *J. Chem. Phys.* **2008**, *129*, 154501.
(14) Shiga, M.; Okazaki, S. *Chem. Phys. Lett.* **1998**, *292*, 431–436.
(15) Mikami, T.; Shiga, M.; Okazaki, S. *J. Chem. Phys.* **2001**, *115*, 9797–9807.
(16) Plattner, N.; Meuwly, M. *Biophys. J.* **2008**, *94*, 2505–2515.
(17) Kumagai, N.; Kawamura, K.; Yokokawa, T. *Mol. Simul.* **1994**, *12*, 177–186.
(18) Montroll, E. W.; Shuler, K. E. *J. Chem. Phys.* **1957**, *26*, 454–464.
(19) Bethe, H. A.; Teller, E. *Ballistic Research Laboratory, Report X-117*, 1941.

(20) Bu, L.; Straub, J. E. *Biophys. J.* **2003**, *85*, 1429–1439.
(21) Zwanzig, R. *J. Chem. Phys.* **1961**, *34*, 1931–1935.
(22) Danielsson, J.; Meuwly, M. *J. Phys. Chem. B* **2007**, *111*, 218–226.
(23) Bader, J. S.; Berne, B. J. *J. Chem. Phys.* **1994**, *100*, 8359–8366.
(24) Stock, G. *Phys. Rev. Lett.* **2009**, *102*, 118301.
(25) Lawrence, C.; Skinner, J. *Proc. Natl. Acad. Sci. U.S.A.* **2005**, *102*, 6720–6725.
(26) Brooks, B. R.; Bruccoleri, R. E.; Olafson, B. D.; States, D. J.; Swaminathan, S.; Karplus, M. *J. Comput. Chem.* **1983**, *4*, 187–217.
(27) Jorgensen, W. L.; Chandrasekhar, J.; Madura, J. D.; Impey, R. W.; Klein, M. L. *J. Chem. Phys.* **1983**, *79*, 926–935.
(28) Nosé, S. *J. Chem. Phys.* **1984**, *81*, 511–519.
(29) Hoover, W. G. *Phys. Rev. A* **1985**, *31*, 1695–1697.
(30) Midda, S.; Das, A. K. *Int. J. Quantum Chem.* **2004**, *98*, 447–455.
(31) Rappé, A. K.; Casewit, C. J.; Colwell, K. S.; Goddard, W. A., III; Skiff, W. M. *J. Am. Chem. Soc.* **1992**, *114*, 10024–10035.
(32) Stone, A. J. *J. Chem. Theory Comput.* **2005**, *1*, 1128–1132.
(33) Frisch, M. J.; *Gaussian 03, Revision B.01*; Gaussian, Inc.: Wallingford, CT, 2003.
(34) Bradforth, S. E.; Kim, E. H.; Arnold, D. W.; Neumark, D. M. *J. Chem. Phys.* **1993**, *98*, 800–810.
(35) Ryckaert, J.-P.; Ciccotti, G.; Berendsen, H. J. C. *J. Comput. Phys.* **1977**, *23*, 327–341.
(36) Yoneya, M.; Berendsen, H. J. C.; Hirasawa, K. *Mol. Simul.* **1994**, *13*, 395–405.
(37) Plattner, N.; Lee, M. W.; Meuwly, M. *Faraday Discuss.* **2010**, *147*, 217–230.
(38) Allen, M. P.; Tildesley, D. J. *Computer Simulation of Liquids*; Oxford University Press: New York, 1987.
(39) Wilson, E. B., Jr.; Decius, J. C.; Cross, P. C. *Molecular Vibrations—The Theory of Infrared and Raman Vibrational Spectra*; McGraw-Hill: New York, 1955.
(40) Lemus, R. *J. Mol. Spectrosc.* **2004**, *225*, 73–92.
(41) Burnham, C. J.; Li, J. C.; Leslie, M. *J. Phys. Chem. B* **1997**, *101*, 6192–6195.
(42) Ikeda-Fukazawa, T.; Horikawa, S.; Hondoh, T.; Kawamura, K. *J. Chem. Phys.* **2002**, *117*, 3886–3896.
(43) Bondi, A. *J. Phys. Chem.* **1964**, *68*, 441–451.
(44) Karasawa, N.; Dasgupta, S.; Goddard, W. A., III *J. Phys. Chem.* **1991**, *95*, 2260–2272.
(45) Venyaminov, S. Y.; Prendergast, F. G. *Anal. Biochem.* **1997**, *248*, 234–245.
(46) Koziński, M.; Garrett-Roe, S.; Hamm, P. *Chem. Phys.* **2007**, *341*, 5–10.
(47) Schmid, F. F.-F.; Meuwly, M. *J. Chem. Theory Comput.* **2008**, *4*, 1949–1958.
(48) Huang, J.; Meuwly, M. *J. Chem. Theory Comput.* **2010**, *6*, 467–476.
(49) Lange, O. F.; van der Spoel, D.; de Groot, B. L. *Biophys. J.* **2010**, *99*, 647–655.